Supplementary Figure 1

A DNMT3B expression in 6DT1 tumors and normal mammary glands

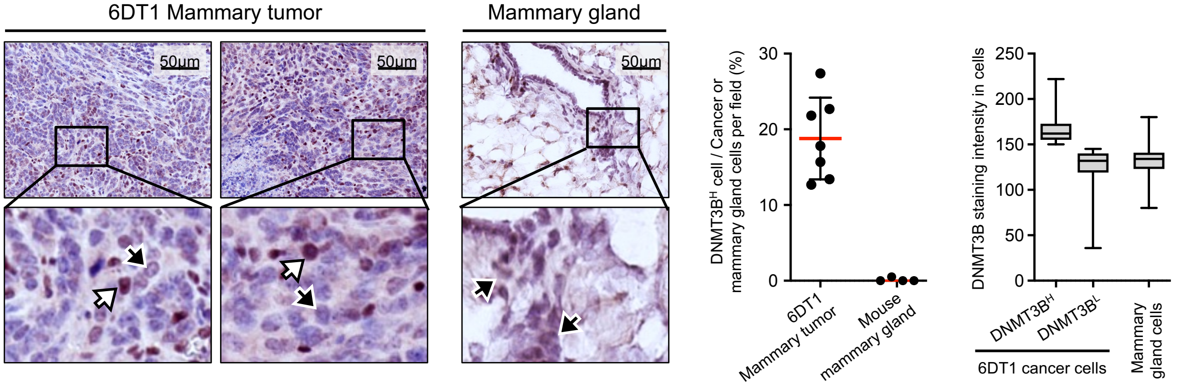

B DNMT3B expression in E-cadherin positive 4T1 cancer cells in tumors

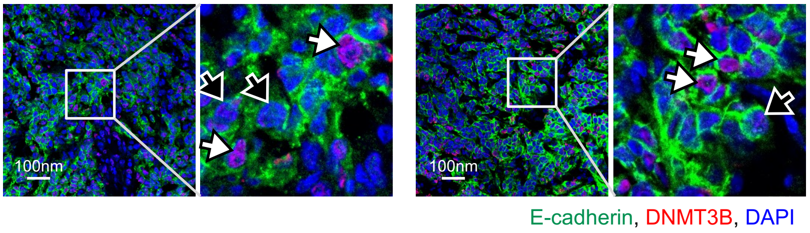

C DNMT3A and DNMT1 expression and patient survival

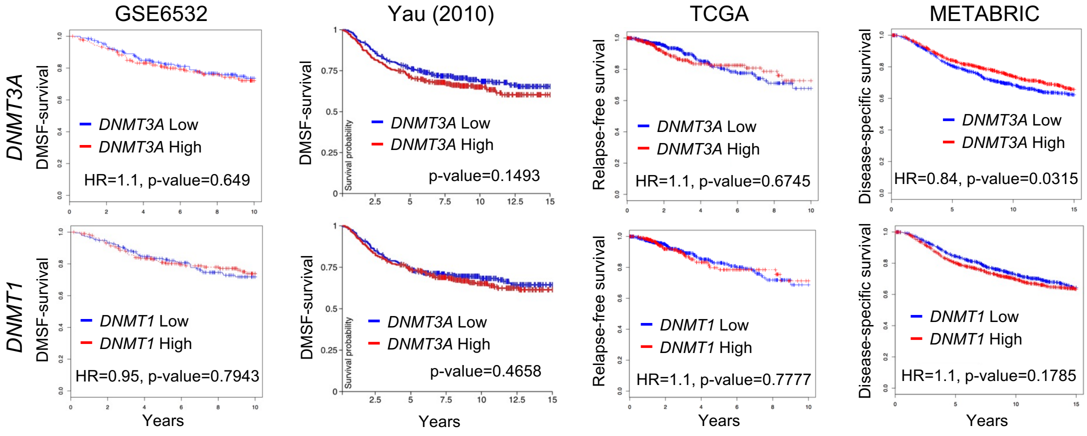

D DNMT3A and DNMT1 expression and tumor stages and subtypes

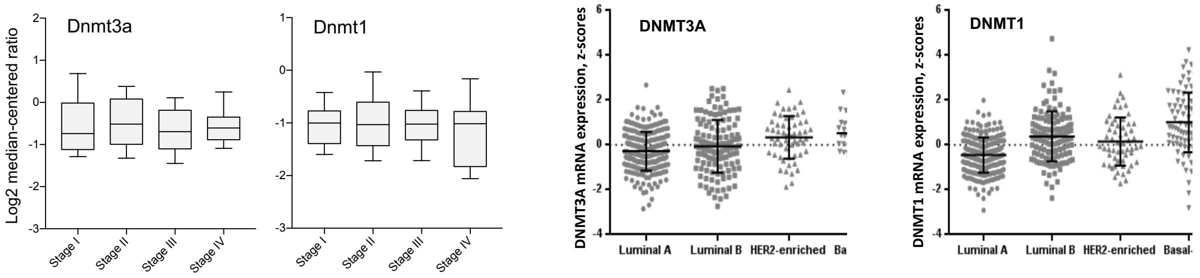

Supplementary Figure 1. A. DNMT3B IHC of 6DT1 mammary tumors and normal mammary glands from BALB/c mice. Percentage of DNMT3B^H cells in cancer and mammary glands cells. Average DNMT3B intensity of DNMT3B^H and DNMT3B^L 6DT1 cancer cells and mammary gland cells on the right panels. Shown are representative images of DNMT3B^H (white arrow) and DNMT3B^L cells (black arrows). **B.** E-cadherin (green) and DNMT3B (red) IF of 4T1 mammary tumors. **C.** Kaplan-Meier plots for correlation DNMT3A (upper panel) or DNMT1 (lower panel) to patient survival in human breast cancer datasets. **D.** DNMT3A and DNMT1 expression levels in breast tumors at different stages (left 2 panels) and with different subtypes (right 2 panels).

Correlation of gene expression and promoter methylation for DNMT3B target genes

Gene	Spearman r
PTPN7	-0.785
INPP5D	-0.599
CLDN4	-0.327
TCF7	-0.31
SFRP1	-0.278
PMEPA1	-0.273
INPP5J	-0.26
NF1	-0.239
CLDN9	-0.229
SOX9	-0.226
CLDN3	-0.118
DUSP4	-0.083
FZD1	-0.03
CDH11	-0.021
LFNG	0.009
TNFAIP3	0.035
SERPINE1	0.058
CLDN5	0.092
WNT7A	0.169

Supplementary Figure 2

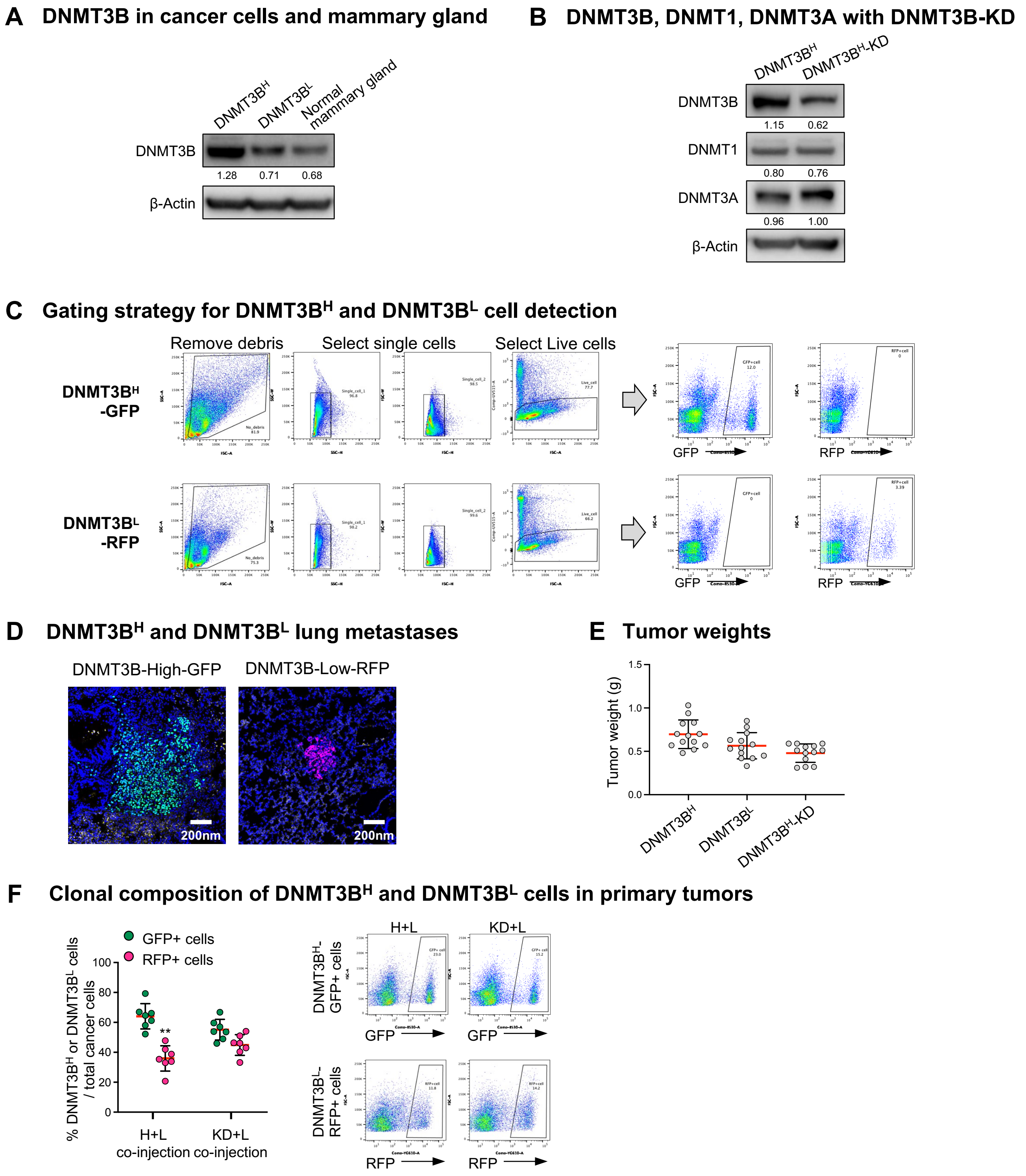

Supplementary Figure 2. A. DNMT3B Western blot for DNMT3B^{H}, DNMT3B^{L} 4T1 cells and normal mammary glands. **B.** DNMT3B, DNMT1 and DNMT3A Western blot for DNMT3B^{H} and DNMT3B^{H}-KD cells. **C.** Gating strategy to detect GFP^{+} and RFP^{+} cells in tissue samples using flow cytometry. **D.** Representative immunofluorescent images of metastatic nodules in the lungs at 4 weeks after injection of mixed DNMT3B^{H}-GFP and DNMT3B^{L}-RFP 4T1 cells. **E.** Weights of primary tumors at week 4. **F.** Flow cytometry of GFP+ and RFP+ cells in primary tumors at 4 weeks after co-injection of DNMT3B^{H}-GFP and DNMT3B^{L}-RFP (H+L) or DNMT3B^{H}-KD-GFP and DNMT3B^{L}-RFP (KD+L) 4T1 cells. Data are presented as mean ± SD. ** $p < 0.01$.

Supplementary Figure 3

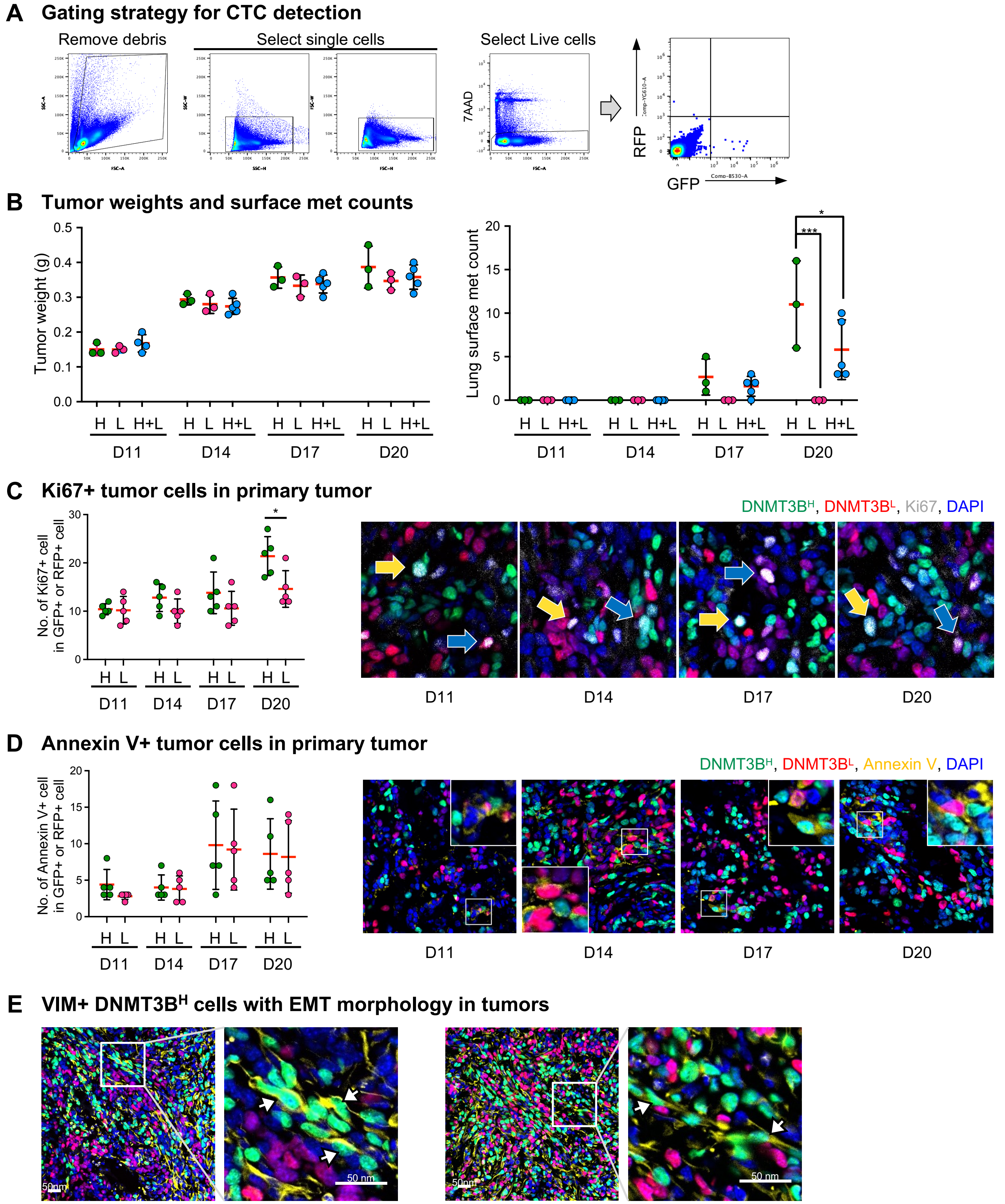

Supplementary Figure 3. **A.** Flow cytometry gating strategy to detect GFP+ and RFP+ CTCs. **B.** Tumor weights and surface metastases (met) counts in the lungs with time course experiment. **C.** Quantitated data and representative images of GFP+ (yellow arrow) and RFP+ (blue arrow) cells with Ki67 expression in primary tumors. **D.** Quantitated data and representative images of GFP+ and RFP+ cells with Annexin V expression in primary tumors. **E.** Representative images of VIM+ DNMT3B^H cells with EMT morphology, indicated by white arrows, in primary tumors. Data are presented as mean ± SD. * $p < 0.05$, *** $p < 0.001$.

Supplementary Figure 4

A DNA methylation levels at Vim gene locus

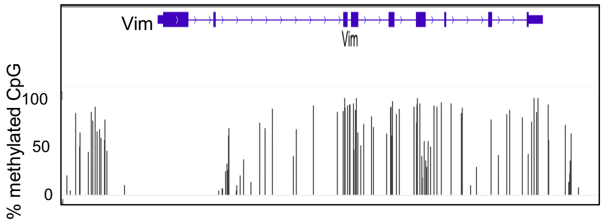

B DNMT3B enrichment at Snai1

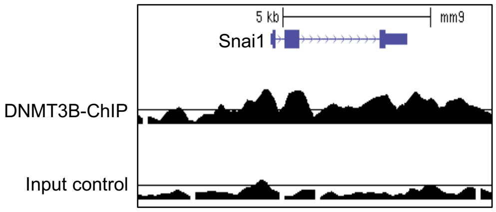

C mRNA expression of methylation-sensitive genes

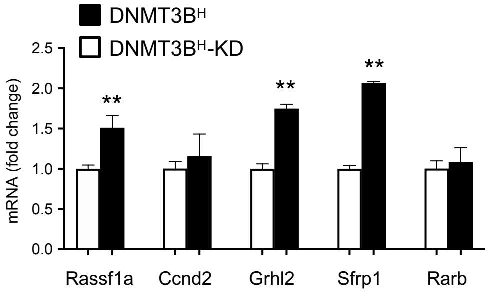

D DNMT3B enrichment at the promoters of Grhl2 and Rassf1a

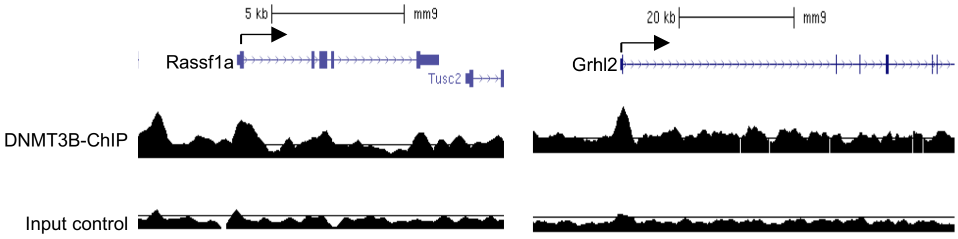

Supplementary Figure 4. **A.** High DNA methylation levels of CpGs in Vim gene body. **B.** DNMT3B enrichment in Snai1 gene body in comparison to input control. **C.** qPCR result showing increased mRNA expression of methylation-sensitive genes, Rassf1a, Grhl2 and Sfrp1, by DNMT3B knockdown in DNMT3B^{H} cells. **D.** DNMT3B enrichment in the promoter regions of Rassf1a and Grhl2 in comparison to input control. Data are presented as mean ± SD. ** $p < 0.01$.